

Jet suppression of pions and single electrons at Au+Au collisions at RHIC

Magdalena Djordjevic¹

¹*Institute of Physics Belgrade, University of Belgrade, Serbia*
(Dated: May 13, 2021)

Jet suppression is considered to be a powerful tool to study the properties of a QCD medium created in ultra-relativistic heavy ion collisions. However, theoretical predictions obtained by using jet energy loss in *static* QCD medium show disagreement with experimental data, which is known as the heavy flavor puzzle at RHIC. We calculate the suppression patterns of pions and single electrons for Au+Au collisions at RHIC by including the energy loss in a finite size *dynamical* QCD medium, with finite magnetic mass effects taken into account. In contrast to the static case, we here report a good agreement with the experimental results, where this agreement is robust with respect to magnetic mass values. Therefore, the inclusion of dynamical QCD medium effects provides a reasonable explanation of the heavy flavor puzzle at RHIC.

PACS numbers: 12.38.Mh; 24.85.+p; 25.75.-q

INTRODUCTION

Jet suppression [1] measurements at RHIC and LHC, and their comparison with theoretical predictions, provide a powerful tool for mapping the properties of a QCD medium created in ultra-relativistic heavy ion collisions [2–4]. However, jet suppression predictions, done under assumption of static QCD medium [5–7], showed a disagreement with the available data from RHIC experiments [8–11]. This disagreement has been named “heavy flavor puzzle at RHIC” [12, 13], and raised important questions about the ability of the available theories to model the matter created at ultra-relativistic heavy ion collisions at RHIC.

Since the suppression results from the energy loss of high energy partons moving through the plasma [14–17], accurate computations of jet energy loss mechanisms are essential for the reliable predictions of jet suppression. In [18, 19], we developed a theoretical formalism for the calculation of radiative energy loss in realistic finite size *dynamical* QCD medium (see also a viewpoint [12]), which abolished a static approximation used in previous models [20–26]. Furthermore, in [27], we extended the study from [18] to include a possibility for existence of finite magnetic mass; this generalization was motivated by various non-perturbative approaches [28–31], which report non-zero magnetic mass. These studies, together with the previously developed collisional energy loss formalism in finite size dynamical QCD medium [32], enable us to provide the most reliable computations of the energy loss in QGP so far.

In this paper, we integrate the developed energy loss formalism into a computational framework that can generate reliable predictions for RHIC and LHC experimental data. The numerical procedure includes: *i*) both collisional and radiative energy loss from the newly developed (dynamical QCD medium) formalism [18, 19, 27, 32], *ii*) multi-gluon fluctuations, i.e. the fact that energy loss is a distribution [33], and *iii*) path length fluctuations,

i.e. the fact that particles travel different paths in the medium [34]. We use this framework to generate suppression predictions for pions and single electrons at most central 200 GeV Au+Au collisions at RHIC. The generated predictions are directly compared with RHIC experimental data [8–11], in order to test our understanding of QGP created at these collisions.

COMPUTATIONAL FRAMEWORK

The quenched spectra of partons, hadrons, and leptons are calculated as in [34, 35] from the generic pQCD convolution

$$\frac{E_f d^3\sigma(e)}{dp_f^3} = \frac{E_i d^3\sigma(Q)}{dp_i^3} \otimes P(E_i \rightarrow E_f) \otimes D(Q \rightarrow H_Q) \otimes f(H_Q \rightarrow e), \quad (1)$$

where Q denotes quarks and gluons. For charm and bottom, the initial quark spectrum, $E_i d^3\sigma(Q)/dp_i^3$, is computed at next-to-leading order using the code from [36, 37]; for gluons and light quarks, the initial distributions are computed at leading order as in [38]. $P(E_i \rightarrow E_f)$ is the energy loss probability, $D(Q \rightarrow H_Q)$ is the fragmentation function of quark or gluon Q to hadron H_Q . The last step ($f(H_Q \rightarrow e)$) is only applicable for heavy quarks, and it represents the decay function of hadron H_Q into the observed single electron. We use the same mass and factorization scales as in [39] and employ the CTEQ5M parton densities [40] with no intrinsic k_T . As in [39] we neglect shadowing of the nuclear parton distribution.

We assume that the final quenched energy E_f is large enough that the Eikonal approximation can be employed. We also assume that in Au+Au collisions, the jet to hadron fragmentation functions are the same as in e^+e^- collisions. This assumption is expected to be valid in the deconfined medium case, where hadronization of

$Q \rightarrow H_Q$ cannot occur until the quark emerges from the QGP.

As in [34], the energy loss probability $P(E_i \rightarrow E_f)$ is generalized to include both radiative and collisional energy loss and their fluctuations. However, a major difference between [34] and the present study is that we here take into account both the radiative [18] and collisional [32] energy losses in a realistic *finite size dynamical* QCD medium.

To take into account geometric path length fluctuations in the energy loss probability, we use [34]:

$$P(E_i \rightarrow E_f = E_i - \Delta_{rad} - \Delta_{coll}) = \int dL P(L) P_{rad}(\Delta_{rad}; L) \otimes P_{coll}(\Delta_{coll}; L). \quad (2)$$

Here $P(L)$ is the distribution of path lengths traversed by hard scatterers in 0-5% most central collisions, in which the lengths are weighted by the probability of production and averaged over azimuth. Note that currently two definitions for $P(L)$ (see [41]), one from [34] and the other from [42], are commonly used. Since these distributions are significantly different (see [41]), we will use both of them in the analysis. Also, since $P(L)$ is a purely geometric quantity, it is the same for all jet varieties.

$P_{rad}(\Delta_{rad}; L)$ and $P_{coll}(\Delta_{coll}; L)$ in Eq. (2) are, respectively, the radiative and collisional energy loss probabilities. The procedure for including fluctuations of the radiative energy loss probability ($P_{rad}(\Delta_{rad}; L)$) due to gluon number fluctuations is discussed in detail in Ref. [35, 43]. Note that the procedure is here generalized to include the radiative energy loss in finite size dynamical QCD medium [18, 19], as well as a possibility for existence of finite magnetic mass [27]; in particular, we extract the gluon radiation spectrum from Eq. (10) in [27]. For collisional energy loss probability ($P_{coll}(\Delta_{coll}; L)$), the full fluctuation spectrum is approximated by a Gaussian centered at the average energy loss with variance $\sigma_{coll}^2 = 2T \langle \Delta E^{coll}(p_\perp, L) \rangle$ [34, 44]. Here $\Delta E^{coll}(p_\perp, L)$ is given by Eq. (14) in [32], T is the temperature of the medium, p_\perp is the initial momentum of the jet, and L is the length of the medium traversed by the jet.

We note that, in the suppression calculations, we separately treat radiative from collisional energy loss; consequently, we first calculate the modification of the quark and gluon spectrum due to radiative energy loss, and then due to collisional energy loss in QCD medium. This is a reasonable approximation when the radiative and collisional energy losses can be considered small (which is in the essence of the soft-gluon, soft-rescattering approximation used in all energy loss calculations so far [18–26, 45]), and when collisional and radiative energy loss processes are decoupled from each other (which is the case in the HTL approach [46] used in our energy loss calculations [18, 19, 32]). Also, we assume that strong coupling constant α_S is fixed at 0.3.

Finally, to obtain π^0 suppression from quark and gluon suppression, we use the following estimate [47, 48]

$$R_{AA}(\pi^0, p_\perp) \approx f_g R_{AA}(g, p_\perp) + (1 - f_g) R_{AA}(l, p_\perp), \quad (3)$$

where $f_g \approx e^{-p_\perp/10.5 \text{ GeV}}$ is the fraction of pions with a given momentum p_\perp that arise from gluon jet fragmentation, $R_{AA}(g, p_\perp)$ is the gluon suppression and $R_{AA}(l, p_\perp)$ is the light quark suppression.

To calculate D and B meson suppression, we will use both delta and Peterson [49] fragmentation functions. Furthermore, to obtain single electron suppression, we will use the following estimate [5]:

$$R_{AA}(e^\pm, p_\perp) \approx \frac{R_{AA}(D, 2p_\perp) \frac{d\sigma_D(2p_\perp)}{dp_\perp} + R_{AA}(B, 2p_\perp) \frac{d\sigma_B(2p_\perp)}{dp_\perp}}{\frac{d\sigma_D(2p_\perp)}{dp_\perp} + \frac{d\sigma_B(2p_\perp)}{dp_\perp}}, \quad (4)$$

where $\frac{d\sigma_D(p_\perp)}{dp_\perp}$ ($\frac{d\sigma_B(p_\perp)}{dp_\perp}$) is D (B) meson initial momentum distribution, and $R_{AA}(D, p_\perp)$ ($R_{AA}(B, p_\perp)$) is the D (B) meson suppression.

NUMERICAL RESULTS

In this section, we concentrate at 200 GeV Au+Au collisions at RHIC, and present our suppression predictions for light and heavy flavor observables. For this, we consider a quark-gluon plasma of temperature $T = 225 \text{ MeV}$, with $N_f = 2.5$ effective light quark flavors and strong interaction strength $\alpha_S = 0.3$, as representative of average conditions encountered in Au+Au collisions at RHIC. For the light quarks we assume that their mass is dominated by the thermal mass $M = \mu/\sqrt{6}$, where $\mu = gT\sqrt{1+N_f/6} \approx 0.5 \text{ GeV}$ is the Debye screening mass. The gluon mass is taken to be $m_g = \mu/\sqrt{2}$. For the charm (bottom) mass we use $M = 1.2 \text{ GeV}$ ($M = 4.75 \text{ GeV}$).

Figure 1 shows momentum dependence of quarks and gluon suppressions at RHIC, obtained by using path length distributions from [34]. We observe a clear hierarchy between the quarks and gluon suppressions: *i*) bottom quark is significantly less suppressed than charm quark; *ii*) charm and light quarks have similar suppressions for initial jet energies larger than 5 GeV; *iii*) gluons are significantly more suppressed than all types of quarks. This already observed/established hierarchy (see e.g. [43]) therefore remains valid for the case of dynamical QCD medium as well, despite the fact that both inclusion of path length fluctuations [34] and dynamical effects [19] into the suppression calculations tend to reduce the difference between different types of quarks and gluons. We also observe that inclusion of magnetic mass can decrease the jet suppression (for all types of quarks and gluons) from 25-50%, compared to the case of zero magnetic mass. While in Fig. 1 we show only the

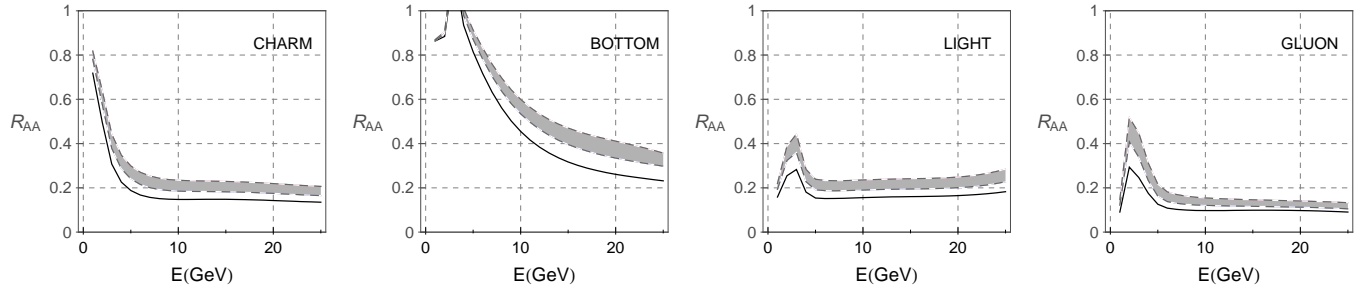


FIG. 1: Quarks and gluon suppressions are presented as a function of initial jet energy for 200 GeV Au+Au collisions at RHIC. The panels are obtained by using path length distributions from [34]. On each panel full curves correspond to the case when magnetic mass is equal to zero. Gray bands correspond to the case when magnetic mass is non-zero (i.e. $0.4 < \mu_M/\mu_E < 0.6$ [28–31]), where the lower boundary corresponds to $\mu_M/\mu_E = 0.4$ and the upper boundary corresponds to $\mu_M/\mu_E = 0.6$.

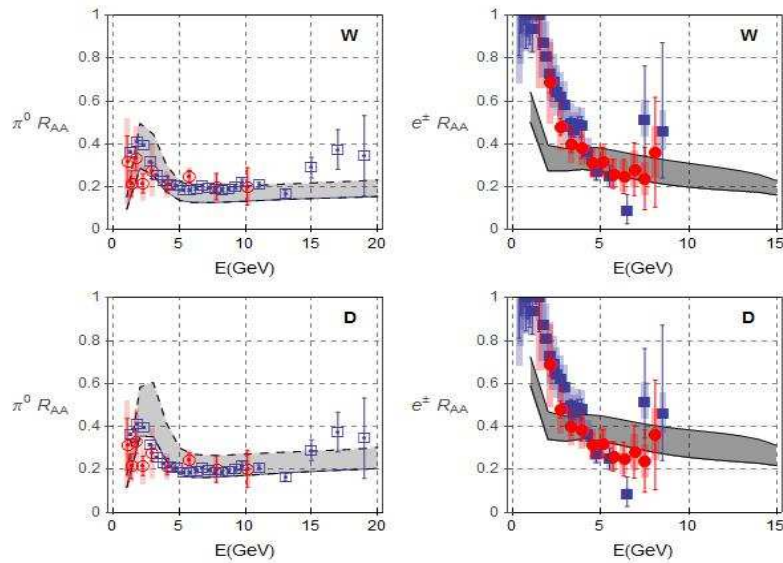


FIG. 2: Left panels show the comparison of pion suppression predictions with π^0 PHENIX [8] and STAR [10] experimental data from 200 GeV Au+Au collisions at RHIC. Right panels show the comparison of single electron suppression predictions with non-photonic single electron data from PHENIX [9] and STAR [11] at 200 GeV Au+Au collisions. For the two upper panels, and the two lower panels, the suppression predictions are obtained, respectively, by using path length distributions from [34] (marked with “W”) and [42] (marked with “D”). On each panel, the gray region corresponds to the case when $\mu_M \geq 0$ (i.e. $0 < \mu_M/\mu_E < 0.6$), where the lower boundary corresponds to $\mu_M/\mu_E = 0$ and the upper boundary corresponds to $\mu_M/\mu_E = 0.6$.

results by using path length distributions from [34], we observe somewhat lower suppression results when distribution from [42] is used (data not shown); this is expected having in mind higher probability for lower path-lengths in [42] compared to [34] (see [41]).

To calculate D and B meson suppression, we used both delta and Peterson [49] fragmentation functions, and observed that the choice of fragmentation function only marginally changes the value of suppression R_{AA} (data not shown). The reason behind the small difference is that fragmentation functions do not significantly modify the distribution slopes [43], due to which the meson suppression becomes insensitive to the choice of fragmentation function. For simplicity, we will therefore further use delta function fragmentation for the calculation of single electron suppression.

Figure 2 shows momentum dependence of pion and single electron suppressions at RHIC, obtained by using two path length distributions (from [34] and from [42]). The predictions are compared with the relevant PHENIX [8, 9] and RHIC [10, 11] experimental data at Au+Au collisions at RHIC. For both path length distributions we

observe a reasonable agreement with the experimental data, which is moreover robust with respect to non-zero magnetic mass introduction.

Furthermore, from Fig. 2 we see that at jet energies above 15 GeV, the predicted pion and single electron suppressions become very similar. This prediction is reasonable, since *i*) at high jet energies suppression patterns for all types of quarks become similar, and *ii*) above 10 GeV pion suppression is strongly dominated by light quark suppression (i.e. gluon contribution to pion suppression becomes negligible) [47, 48]. This behavior is qualitatively different from the one below 10 GeV, where obtained suppressions are notably different (by $\lesssim 2$). It will be interesting to compare this predicted pattern with the upcoming high luminosity RHIC data.

CONCLUSIONS

In this paper we calculated the suppression pattern of pions, D and B mesons and single electrons in central 200 GeV Au+ Au collisions at RHIC energies. The

calculation is based on the radiative and collisional energy loss in a finite size dynamical QCD medium, which is a key ingredient for obtaining reliable predictions for jet quenching in ultra-relativistic heavy ion collisions. This energy loss formalism was here integrated into a computational framework that includes multi-gluon and path length fluctuations. We obtained a reasonably good agreement between the generated suppression patterns and experimental data at Au+Au collisions at RHIC, and this agreement is robust with respect to introduction of finite magnetic mass. The agreement strongly suggests that the main deficiency responsible for the “heavy flavor puzzle” at RHIC was the *static* approximation, i.e. the fact that dynamical nature of plasma constituents was not taken into account. Predictions of the dynamical energy loss formalism remain to be tested against the upcoming high luminosity RHIC and LHC data.

Acknowledgments: This work is supported by Marie Curie International Reintegration Grant within the 7th European Community Framework Programme (PIRG08-GA-2010-276913) and by the Ministry of Science and Technological Development of the Republic of Serbia, under projects No. ON171004 and ON173052.

-
- [1] J.D. Bjorken: FERMILAB-PUB-82-059-THY (1982).
 [2] N. Brambilla et al., Preprint hep-ph/0412158 (2004).
 [3] M. Gyulassy, Lect. Notes Phys. **583**, 37 (2002).
 [4] D. d’Enterria, B. Betz, Lect. Notes Phys. **785**, 285 (2010).
 [5] M. Djordjevic, M. Gyulassy, S. Wicks and R. Vogt, Phys. Lett. B **632**, 81 (2006).
 [6] R. Rapp, V. Greco and H. van Hees, Nucl. Phys. A **774**, 685 (2006).
 [7] N. Armesto, A. Dainese, C. A. Salgado and U. A. Wiedemann, Phys. Rev. D **71**, 054027 (2005).
 [8] A. Adare *et al.* [PHENIX collaboration], Phys. Rev. Lett. **101**, 232301 (2008).
 [9] A. Adare *et al.* [PHENIX collaboration], Phys. Rev. Lett. **98**, 172301 (2007).
 [10] B.I. Abelev *et al.* [STAR collaboration], Phys. Rev. C **80** 44905 (2009).
 [11] B.I. Abelev *et al.* [STAR collaboration], Phys. Rev. Lett. **98**, 192301 (2007).
 [12] M. Gyulassy, Physics **2**, 107 (2009).
 [13] M. Djordjevic, J. Phys. G **32**, S333 (2006).
 [14] M. Gyulassy, I. Vitev, X. N. Wang and B. W. Zhang, in Quark Gluon Plasma 3, edited by R. C. Hwa and X. N. Wang, p. 123 (World Scientific, Singapore, 2003)
 [15] R. Baier, Yu. L. Dokshitzer, A. J. Mueller and D. Schiff, Phys. Rev. C **58**, 1706 (1998).
 [16] R. Baier, D. Schiff, B. G. Zakharov, Ann. Rev. Nucl. Part. Sci. **50**, 37 (2000).
 [17] A. Kovner and U. A. Wiedemann, in *Quark Gluon Plasma 3*, edited by R.C. Hwa and X.N. Wang, p. 192 (World Scientific, Singapore, 2003).
 [18] M. Djordjevic, Phys. Rev. C **80**, 064909 (2009).
 [19] M. Djordjevic and U. Heinz, Phys. Rev. Lett. **101**, 022302 (2008).
 [20] M. Djordjevic and M. Gyulassy, Phys. Lett. B **560**, 37 (2003); and Nucl. Phys. A **733**, 265 (2004).
 [21] M. Gyulassy, P. Levai and I. Vitev, Nucl. Phys. B **594**, 371 (2001).
 [22] M. Gyulassy and X. N. Wang, Nucl. Phys. B **420**, 583 (1994); X. N. Wang, M. Gyulassy and M. Plumer, Phys. Rev. D **51** (1995) 3436.
 [23] U.A. Wiedemann, Nucl. Phys. B **588**, 303 (2000); and Nucl. Phys. B **582**, 409 (2000).
 [24] E. Wang and X. N. Wang, Phys. Rev. Lett. **87** 142301, (2001). X. N. Wang and X. F. Guo, Nucl. Phys. A **696**, 788 (2001); X. F. Guo and X. N. Wang, Phys. Rev. Lett. **85** 3591, (2000).
 [25] N. Armesto, C. A. Salgado and U. A. Wiedemann, Phys. Rev. D **69**, 114003 (2004).
 [26] M. Djordjevic, Phys. Rev. C **73**, 044912 (2006).
 [27] M. Djordjevic, arXiv:1105.4359 [nucl-th]
 [28] Yu. Maezawa et al. [WHOT-QCD Collaboration], Phys. Rev. D **81** 091501 (2010); Yu. Maezawa et al. [WHOT-QCD Collaboration], PoS Lattice 194 (2008).
 [29] A. Nakamura, T. Saito and S. Sakai, Phys. Rev. D **69**, 014506 (2004).
 [30] A. Hart, M. Laine and O. Philipsen, Nucl. Phys. B **586**, 443 (2000).
 [31] D. Bak, A. Karch and L. G. Yaffe, JHEP **0708**, 049 (2007).
 [32] M. Djordjevic, Phys. Rev. C **74**, 064907 (2006).
 [33] M. Gyulassy, P. Levai and I. Vitev, Phys. Lett. B **538**, 282 (2002).
 [34] S. Wicks, W. Horowitz, M. Djordjevic and M. Gyulassy, Nucl. Phys. A **784**, 426 (2007).
 [35] M. Djordjevic, M. Gyulassy, R. Vogt and S. Wicks, Phys. Lett. B **632** 81 (2006).
 [36] M. Cacciari, P. Nason and R. Vogt, Phys. Rev. Lett. **95** 122001 (2005).
 [37] M. L. Mangano, P. Nason and G. Ridolfi, Nucl. Phys. B **373**, 295 (1992).
 [38] I. Vitev and M. Gyulassy, Phys. Rev. Lett. **89**, 252301 (2002).
 [39] R. Vogt, Int. J. Mod. Phys. E **12**, 211 (2003).
 [40] H. L. Lai *et al.* [CTEQ Collaboration], Eur. Phys. J. C **12**, 375 (2000).
 [41] S. Wicks, PhD thesis, AAT-3333486, PROQUEST-1614268891, 2008. 338pp
 [42] A. Dainese, Eur. Phys. J. C **33** 495 (2004).
 [43] M. Djordjevic, M. Gyulassy and S. Wicks, Phys. Rev. Lett. **94**, 112301 (2005).
 [44] G. D. Moore, D. Teaney, Phys. Rev. C **71**, 064904 (2005).
 [45] P. Arnold, G. D. Moore and L. G. Yaffe, JHEP **0111**, 057 (2001); JHEP **0206**, 030 (2002); JHEP **0301**, 030 (2003).
 [46] M. Djordjevic, Nucl. Phys. A **783** 197 (2007).
 [47] I. Vitev, Phys. Lett. B **606**, 303 (2005).
 [48] A. Adil and M. Gyulassy, Phys. Lett. B **602** (2004) 52.
 [49] C. Peterson, D. Schlatter, I. Schmitt and P. M. Zerwas Phys. Rev. D **27**, 105 (1983).